

Daochi Chengqi Decoction Reverses the Acute Phase Progression of Epidemic Febrile Disease in Rats by Inhibiting Mitochondrial Oxidative Damage

SHENGLU LIN*, DEZHI CHEN¹, BIRONG ZHENG, QIAOHUI CHEN¹, WEIXIA ZHUANG² AND HUILING YU³

Department of Pharmacy, Fujian Medical University Union Hospital, Fuzhou, Fujian 350001, ¹Department of Pharmacy, 910th Hospital of PLA, Quanzhou, Fujian 362000, ²Department of Pharmacy, The First Affiliated Hospital of Fujian Medical University, Fuzhou, Fujian 350005, ³Department of Pharmacy, Fujian Provincial Geriatric Hospital, Fuzhou, Fujian 350009, China

Lin *et al.*: Daochi Chengqi Decoction in Treatment of Epidemic Febrile Disease

We aimed to evaluate the effect of Daochi Chengqi decoction on reversing acute heart and liver injury in rats with summer-heat syndrome of epidemic febrile disease. The Daochi Chengqi decoction-containing serum was prepared by the intragastric administration of Sprague-Dawley rats, and then prepared into complete medium with basal medium for cell intervention. The effects of Daochi Chengqi decoction on the viability of myocardial cells H9C2 and liver cells BRL3A in rats injured by high temperature were detected by cell counting kit-8 assay. Forty Sprague-Dawley rats were randomly divided into negative control group, epidemic febrile disease model group, low-dose Daochi Chengqi decoction group (1 mg/kg), middle-dose Daochi Chengqi decoction group (2 mg/kg) and high-dose Daochi Chengqi decoction group (4 mg/kg). With increasing concentration of Daochi Chengqi decoction, both exhaustion time and movement distance increased, and the body temperature reduced ($p < 0.05$). The mean mitochondrial membrane potential, calcium ions concentration and superoxide dismutase activity in myocardial and liver cells significantly dropped in the model group compared to those in the negative group, and they all rose with increasing concentration of Daochi Chengqi decoction ($p < 0.05$). The messenger ribonucleic acid and protein expressions of toll-like receptor 4, nuclear factor-kappa B and p53 in myocardial and liver cells were significantly higher in the model group than those in the negative group ($p < 0.01$), and they declined with increasing concentration of Daochi Chengqi decoction ($p < 0.05$). Daochi Chengqi decoction can relieve mitochondrial oxidative damage by inhibiting the activity of the toll-like receptor 4/nuclear factor-kappa B signaling pathway.

Key words: Decoction, mitochondrion, oxidative damage, summer-heat syndrome

Summer-heat syndrome is a disease of water loss and electrolyte imbalance caused by high temperature, primarily manifested as body temperature elevation, accompanied by headache, dizziness, nausea, vomiting and other gastrointestinal symptoms^[1]. It can also induce nervous system damage, including convulsion, confusion and coma, and even irreversible damage to the heart, kidney, liver and other organs in severe cases^[2]. When summer-heat syndrome occurs, corresponding responses including heat shock response, oxidative stress response and inflammatory response to heat stimulation will be triggered in the body, and in severe cases, endogenous heat shock protein will be released, excessive free radicals will be produced

and apoptosis will be initiated, thus damaging myocardial and liver cells^[3,4]. In myocardial cells, hyperthermia may lead to Calcium (Ca^{2+}) ions loss or overload in mitochondria, and thus triggers the activation of calmodulin-dependent protein kinases in myocardial cells and causes apoptosis of myocardial cells^[5]. In liver cells, hyperthermia can lead to intracellular mitochondrial dysfunction, and cause lipid peroxidation, protein denaturation and apoptosis of liver cells through a series of oxidative

This is an open access article distributed under the terms of the Creative Commons Attribution-NonCommercial-ShareAlike 3.0 License, which allows others to remix, tweak, and build upon the work non-commercially, as long as the author is credited and the new creations are licensed under the identical terms

*Address for correspondence
E-mail: linshenglu11@163.com

Accepted 08 September 2023
Revised 04 December 2022
Received 25 November 2021
Indian J Pharm Sci 2023;85(5):1257-1267

stress processes^[6]. Daochi Chengqi decoction is a classical Chinese medicine prescription composed of *Radix Paeoniae rubra*, *Radix Rehmanniae*, *Radix et Rhizoma rhei*, *Rhizoma coptidis*, etc., which can eliminate heat accumulation and clear away heat in the small intestine. According to the theory of traditional Chinese medicine, summer-heat syndrome results from deficiency of primordial qi and disharmony between nutrient qi and defensive qi due to accumulation of damp-heat. Daochi Chengqi decoction has the effects of clearing away heat and toxic materials, dredging and dispersing exterior evil, eliminating dampness and alleviating water retention, so it can be used to treat dizziness, headache, thirst, body fever, nausea and vomiting caused by summer-heat syndrome^[7], but its specific molecular mechanism remains unclear. Therefore, the specific mechanism of Daochi Chengqi decoction in reversing the acute phase progression of summer-heat syndrome of epidemic febrile disease in rats was explored in this study, aiming to provide valuable experimental evidence for its rational clinical application.

MATERIALS AND METHODS

Cells and reagents:

Rat myocardial cells H9C2 and liver cells BRL3A (Cell Bank of China Academy of Sciences, China), Specific Pathogen-Free (SPF) grade male Sprague-Dawley (SD) rats (Shanghai SLAC Laboratory Animal Co., Ltd., Shanghai, China, laboratory animal production license No. SCXK (Shanghai) 2008-0016), Roswell Park Memorial Institute (RPMI) 1640 medium, fetal bovine serum and penicillin/streptomycin (Gibco, United States of America (USA)), Cell Counting Kit-8 (CCK-8) assay kit (Vazyme Biotech, Nanjing, China), Bicinchoninic Acid (BCA) protein quantitation kit, RIPA lysis buffer and 4× protein loading buffer (Wuhan ABclonal Biotechnology Co., Ltd., China), Sodium Dodecyl Sulfate-Polyacrylamide Gel Electrophoresis (SDS-PAGE) gel preparation kit and TRIzol reagent (ACROBiosystems, Beijing, China), primary antibodies against Toll-Like Receptor 4 (TLR4) (#14358), Nuclear Factor-Kappa B (NF-κB) (#69994), p53 (#48818), Peroxisome Proliferator-Activated Receptor-Gamma Coactivator 1 (PGC-1) (#2178) and Glyceraldehyde-3-Phosphate Dehydrogenase (GAPDH) (#92310) (cell signaling technology, USA), and *Radix Paeoniae rubra*, *Radix*

Rehmanniae, *Radix et Rhizoma rhei*, *Rhizoma coptidis*, *Cortex phellodendri*, and *Natrii Sulfas* (Pharmacy of Affiliated Hospital of Nanjing University of Traditional Chinese Medicine).

Preparation of Daochi Chengqi decoction-containing serum:

Daochi Chengqi decoction was prepared by decocting in the pharmacy department of our hospital. The filtrate was concentrated to the crude drug mass concentration of 6.12 g/ml and vacuum-dried. Then the concentrated extract was freeze-dried to obtain the Daochi Chengqi decoction extract. The content of the main components was measured by High-Performance Liquid Chromatography (HPLC), and the purity was 99 %. When used, the dry powder of Daochi Chengqi decoction was dissolved in Phosphate Buffered Saline (PBS) into solution. 24 male SD rats were randomly divided into control group, low-dose group, middle-dose group and high-dose group. According to the principle of human equivalent dose for rats, the rats in low-dose group, middle-dose group and high-dose group were treated with 1.16 g/ml, 2.32 g/ml and 4.64 g/ml Daochi Chengqi decoction by gavage, respectively, while those in control group were given the same volume of normal saline by gavage. The drug was administered for 3 consecutive days at 8:00 a.m. and 6:00 p.m. each day. 2 h after the end of the last administration, the rats were anesthetized, and the sterile blood was drawn from the abdominal aorta. After sedimentation, centrifugation and inactivation in a 56° water bath, the blood was stored at -20°. When used, drug-containing serum was added to RPMI 1640 medium to prepare into low-dose, middle-dose and high-dose 10 % drug-containing serum medium for cell treatment. All standardized operations were conducted in accordance with the guidelines formulated by National Medical Products Administration. All animal experiments met the guidelines and requirements of the Ethics Committee of our hospital.

Establishment of rat model of summer-heat syndrome:

Forty SPF-grade SD rats were randomly divided into Negative Control (NC) group, epidemic febrile disease model group (model group), low-dose Daochi Chengqi decoction group (low group, 1 mg/kg), middle-dose Daochi Chengqi decoction

group (middle group, 2 mg/kg) and high-dose Daochi Chengqi decoction group (high group, 4 mg/kg), with eight rats in each group. The rats in NC group were routinely fed. In model group, under the room temperature of 45°, the rats were allowed to run on the treadmill at 25 rpm until they were exhausted. In low, middle and high groups, the rats were treated in the same way as model group, and Daochi Chengqi decoction (1 mg/kg, 2 mg/kg, and 4 mg/kg) was given by gavage at the time of exhaustion. At 3 h after treatment, the rats were sacrificed and the experiment was terminated.

F-actin staining:

H9C2 and BRL3A cells in the logarithmic growth phase were prepared into single cell suspension, and 200 µl of suspended cells were added at a density of 1×10^5 /ml into a 24-well plate with cover glasses laid in advance. After 24 h of treatment with complete medium containing different concentrations of Daochi Chengqi decoction, the cells were fixed with 4 % paraformaldehyde for 30 min at room temperature, permeabilized with 0.5 % Triton X-100 for 5 min and blocked with bovine serum albumin for 1 h at room temperature, followed by F-actin staining with Alexa Fluor® 488 Phalloidin for 1 h. Then the cells were counterstained with 4 mg/ml 4,6-Diamino-2-Phenylindole (DAPI), and the cytoskeleton morphology was immediately observed under a fluorescence microscope.

Transmission electron microscopy:

Upon reaching 85 % confluency of H9C2 and BRL3A cells, intervention modeling was performed. Specifically, after centrifugation at $2000 \times g$ for 5 min, the cells were collected, fixed with 2.5 % glutaraldehyde at room temperature for 30 min away from light, dehydrated, embedded and sliced into ultrathin sections. Finally, the mitochondrial morphology was observed under a transmission electron microscope.

CCK-8 assay:

Cell viability was detected using CCK-8 assay kit. After intervention modeling of H9C2 and BRL3A cells (5×10^3 /ml), 10 µl of CCK-8 reagent was added into each well, and after incubation at 37° in an incubator for 1 h, the Optical Density (OD) value was measured at 450 nm using a microplate reader.

Reverse Transcription-quantitative Polymerase Chain Reaction (RT-qPCR):

Total Ribonucleic Acid (RNA) was extracted from H9C2 and BRL3A cells using RNA extraction kit. According to the manufacturer's instructions, the total RNA was reversely transcribed into complementary Deoxyribonucleic Acid (cDNA) and amplified using PrimeScript RT Master Mix (TaKaRa, Osaka, Japan) and SYBR Premix Ex Taq Kit (TaKaRa, Osaka, Japan). With GAPDH as an internal reference gene, the relative expression of messenger RNA (mRNA) was calculated by $2^{-\Delta\Delta Ct}$ method. The primer sequences are shown in Table 1.

Western blotting:

After intervention modeling of H9C2 and BRL3A cells, they were lysed with lysis buffer. The cell lysates were then centrifuged at 4° and 14 000 rpm for 15 min and the supernatants were collected for protein quantification using the BCA Protein Quantification Kit. Following SDS-PAGE, the extracted proteins were transferred onto a Polyvinylidene Fluoride (PVDF) membrane, soaked in 5 % skim milk for 2 h to block non-specific binding sites, and incubated overnight at 4° with primary antibodies against TLR4 (1:1000), NF-κB (1:1000), p53 (1:1000), PGC-1 (1:1000) and GAPDH (1:2000). After washing, the membrane was incubated again with the corresponding peroxidase-conjugated secondary antibodies for 2 h, and the bands were detected using an enhanced Chemiluminescence system, with GAPDH as an internal reference.

TABLE 1: PRIMER SEQUENCES

Gene	Forward	Reverse
TLR4	5'-CAGGAAACAGCTATGACCM-3'	5'-TGTAACACGACGGCCAGT-3'
NF-κB	5'-CCTCGCCTTTGCCGATCC-3'	5'-GGATCTATCTCATGAGGT-3'
p53	5'-ATACGACTCACTATAGGG-3'	5'-ATTTAGGTGACACTATAG-3'
PGC-1	5'-CAGGAAACAGCTATGACC-3'	5'-TGTAACACGACGGCCAGT-3'
GAPDH	5'-AACCATCTC GCAAT AA-3'	5'-ACGCACAGAATC TAGCG-3'

Enzyme-Linked Immunosorbent Assay (ELISA):

The levels of Tumor Necrosis Factor-Alpha (TNF- α), Interleukin (IL)-6 and IL-1 beta (β) in H9C2 and BRL3A cells were detected using the high-sensitivity ELISA kit. To be specific, 100 μ l of cell culture supernatant was added to the plate, incubated and washed, and then the antibodies against TNF- α , IL-6 and IL-1 β (1:100) were added. After washing, 100 μ l of horseradish peroxidase-labeled streptavidin (1:100) was added to each well. After washing, 100 μ l of chromogenic substrate 3,3',5,5'-Tetramethylbenzidine (TMB) was added to each well for incubation away from light for 10 min, and the reaction was terminated by adding 100 μ l of stop buffer in each well. Finally, the OD values at 450 nm and 570 nm were measured with a microplate reader.

Measurement of Reactive Oxygen Species (ROS) and Malondialdehyde (MDA) levels:

The ROS content in H9C2 and BRL3A cells was measured using ROS assay kit. Specifically, the cells were inoculated into a 12-well plate and cultured until reaching 85 % confluency before intervention modeling. After washing with PBS, 1 ml of 10 μ M Dichlorodihydrofluorescein Diacetate (DCFH-DA) working solution was added to each well, and the cells were incubated in an incubator at 37° away from light for 30 min. Then the cells were washed twice with serum-free medium, and observed and photographed under a fluorescence microscope. After ultra-sonication, H9C2 and BRL3A cells were collected, and 300 μ l of MDA working solution and 100 μ l of samples were mixed, heat-preserved in a 100° water bath for 60 min, and cooled in an ice bath, followed by centrifugation at 10 000 \times g and room temperature for 10 min. Finally, 200 μ l of supernatant was added to a 96-well plate, and the OD values were measured at 532 nm and 600 nm.

Measurement of Mitochondrial Membrane Potential (MMP) and mitochondrial Respiratory Control Ratio (RCR):

MMP was measured by the fluorescent probe Tetramethylrhodamine (TMRM). H9C2 and BRL3A cells isolated were incubated in HEPES buffer for 30 min and washed for 15 min, and then Mean Fluorescence Intensity (MFI) was analyzed by flow cytometry. Mitochondrial RCR is a general

measure of mitochondrial function, with higher levels indicating better mitochondrial function. Before detection, the cells were incubated with GENMED reagent A, and substrate solutions reagent B and reagent C were added in the appropriate order, followed by RCR determination.

Measurement of free Ca²⁺ concentration and ROS in mitochondria:

Preparation of mitochondrial suspension: Tissue samples were centrifuged at 15 000 g for 10 min using a centrifuge, and after the supernatant was discarded, the pellet was suspended in an appropriate buffer and centrifuged again for 15 min, and the supernatant containing mitochondria was collected. Then, the mitochondrial suspension was placed in a test tube and mixed well with Ca²⁺ fluorescent probe or ROS fluorescent probe. Then the fluorescence signal of the fluorescent probe was observed under the excitation wavelength. Mitochondria containing Ca²⁺ or ROS had significantly enhanced fluorescence signals, while mitochondria without Ca²⁺ or ROS had no significant changes in fluorescence signals. The fluorescence signal was detected by flow cytometry, based on which the concentration of Ca²⁺ or ROS in mitochondria was calculated.

Statistical analysis:

All assays were independently repeated at least three times, and Statistical Package for the Social Sciences (SPSS) 20.0 software was used for statistical analysis. The measurement data were described by mean \pm standard deviation. One-way analysis of variance was used for comparison among groups, and the Least Significant Difference (LSD)-t test was performed for pairwise comparison. $p < 0.05$ was considered statistically significant.

RESULTS AND DISCUSSION

To explore the suitable temperature and time of heat exposure, H9C2 and BRL3A cells were incubated in an incubator at different temperatures (37°, 41°, 43° and 45°) for 2 h, and the changes in cell morphology and cell viability were observed. At 37°, H9C2 cells were long spindle-shaped and BRL3A cells were triangle-shaped. At 41° and 43°, the cytoskeleton structure of H9C2 and BRL3A cells began to deform gradually and abnormal morphology emerged. At 45°, H9C2 and BRL3A

cells showed an irregular saccular shape (fig. 1A). The results of CCK-8 assay showed that the viability of H9C2 and BRL3A cells declined gradually with the increase in intervention temperature ($p < 0.01$) (fig. 1B). Furthermore, H9C2 and BRL3A cells were cultured in an incubator at 43° for different time (1 h, 2 h, 3 h and 5 h). The results showed that with the increase in intervention time, the cell morphology began to change from a long spindle shape to an irregular saccular or oval shape (fig. 1C), and the cell viability gradually declined ($p < 0.05$) (fig. 1D). These results suggest that thermal injury can induce changes in morphology and viability of H9C2 and BRL3A cells in a temperature- and time-dependent manner.

H9C2 and BRL3A cells were incubated in an incubator at 43° for 2 h, and then recovered at 37° for different time (0 h, 1 h, 3 h and 5 h). The results of RT-qPCR and Western blotting showed that the mRNA and protein expressions of TLR4, NF- κ B and p53 were significantly increased in H9C2 and BRL3A cells at 0 h and 3 h after recovery from heat exposure compared with those in NC group ($p < 0.01$) (fig. 2A and fig. 2B). At the same time, it was found by ELISA that the levels of inflammatory factors TNF- α , IL-6 and IL-1 β in H9C2 and BRL3A cells were significantly increased at 0 h and 3 h after recovery from heat exposure ($p < 0.001$) (fig. 2C). The above results suggest that at 0 h and 3 h after recovery from heat exposure, the TLR4/NF- κ B signaling pathway is

significantly activated and inflammatory factors are significantly increased in H9C2 and BRL3A cells.

The rats in model group had significantly shorter exhaustion time and movement distance, and significantly higher body temperature than those in NC group ($p < 0.05$). With the increase in the concentration of Daochi Chengqi decoction, both exhaustion time and movement distance were gradually increased, and the body temperature gradually declined ($p < 0.05$) (fig. 3A). As shown in fig. 3B, high temperature caused morphological changes in the mitochondrial structure in myocardial and liver cells. In model group, myocardial and liver cells were obviously swollen, mitochondrial myelin was destroyed, cristae matrix granules disappeared, and highly bright areas were formed in mitochondrial matrix or concentric cristae. With the increase in the concentration of Daochi Chengqi decoction, the damage to the mitochondrial structure of myocardial and liver cells in rats was gradually relieved compared with that in model group. Mitochondria are the key organelles that regulate cell death, and MMP is closely related to mitochondrial function. Compared with that in NC group, the mean MMP of myocardial and liver cells decreased by about (64.3 % \pm 7.9 %) and (68.2 % \pm 8.2 %), respectively, in model group. With the increase in the concentration of Daochi Chengqi decoction, the MMP of myocardial and liver cells in rats gradually increased ($p < 0.05$) as shown in fig. 3C and fig. 3D.

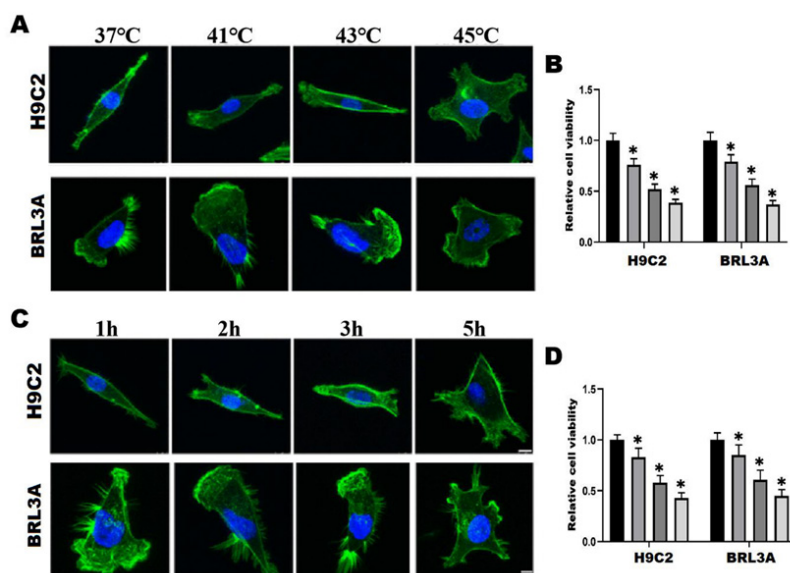


Fig. 1: High temperature caused damage to H9C2 and BRL3A cells in a time- and temperature-dependent manner

Note: * $p < 0.05$, (B) (■): 37°; (□): 41°; (▨): 43° and (▩): 45°, and (D) 1 h; (■): 2 h; (□): 3 h; 4 h; (▨) and (▩): 5 h

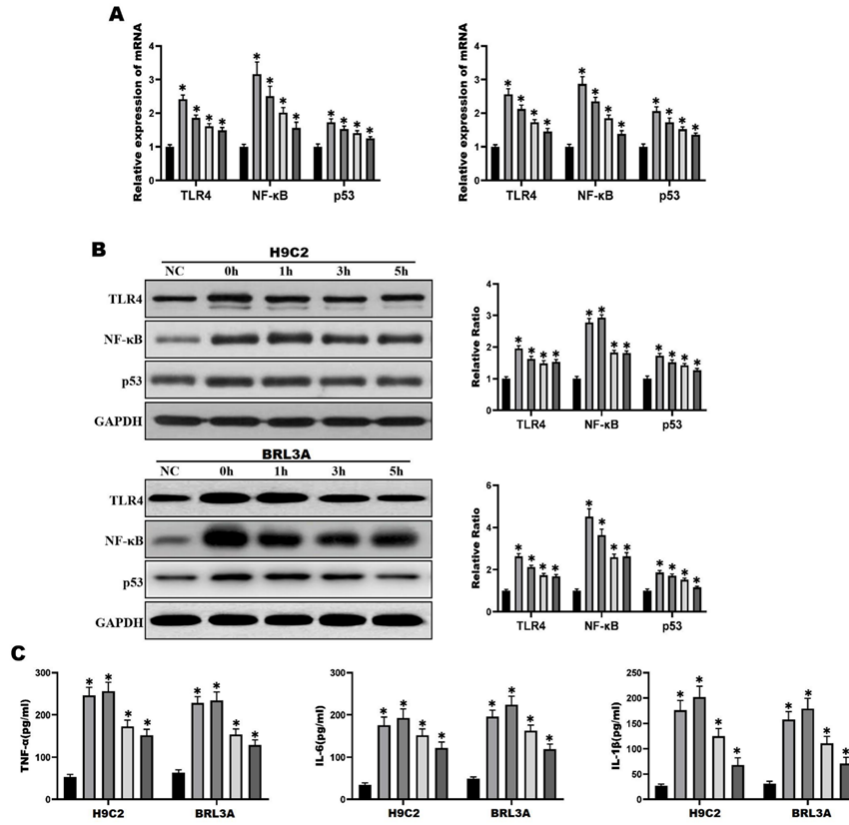


Fig. 2: Thermal injury activated TLR4/NF-κB signaling pathway in myocardial and liver cells
 Note: *p<0.05, (■): NC; (▨): 0 h; (▩): 1 h; (▪): 3 h and (▫): 5 h

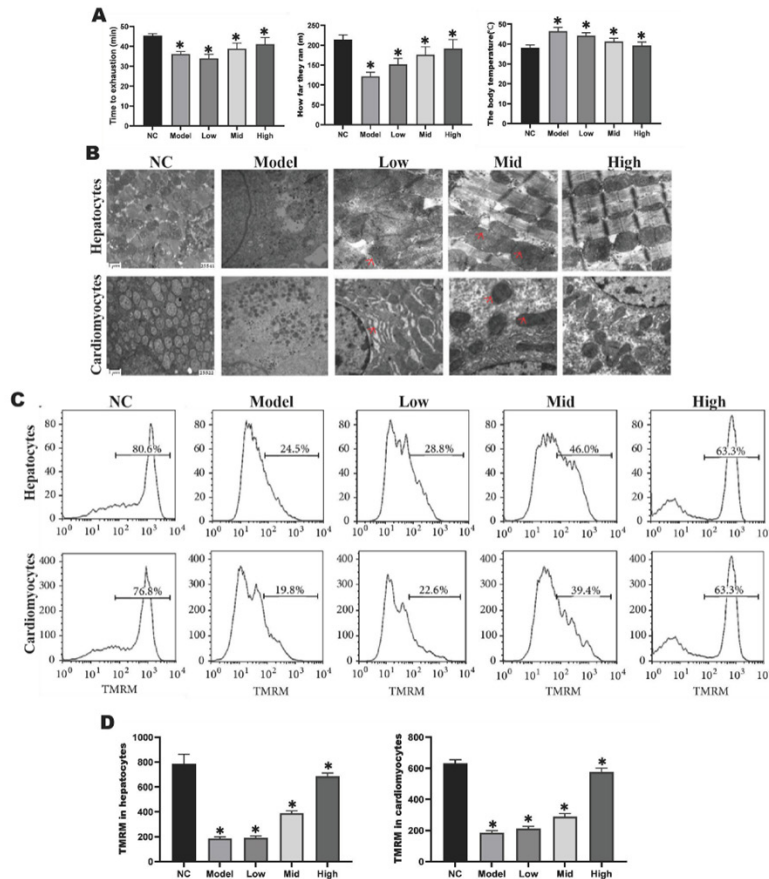


Fig. 3: Daochi Chengqi decoction significantly alleviated the mitochondrial lesions in myocardial and liver cells of rats
 Note: *p<0.05

RCR can be used as an index for the degree of oxidative phosphorylation coupling, and the absorption and release of Ca^{2+} have significant effects on mitochondrial function and metabolic process. The RCR and Ca^{2+} concentration in myocardial and liver cells were significantly lower in model group than those in NC group ($p < 0.05$), while they gradually rose with the increase in the concentration of Daochi Chengqi decoction ($p < 0.05$) (fig. 4).

To study the effect of Daochi Chengqi decoction on mitochondrial ROS in rat myocardial and liver cells, the ROS levels in liver cells and myocardial cells were detected using ROS-specific fluorescent probes. The mitochondrial ROS production in myocardial and liver cells was significantly higher in model group than that in NC group ($p < 0.05$), while it gradually declined with the increase in the concentration of Daochi Chengqi decoction ($p < 0.05$) as shown in fig. 5.

The results of ELISA revealed that compared with NC group, model group had significantly decreased Superoxide Dismutase (SOD) activity in

mitochondria ($p < 0.05$) and significantly increased MDA activity ($p < 0.05$). With the increase in the concentration of Daochi Chengqi decoction, the SOD activity in mitochondria of myocardial and liver cells gradually rose, and the MDA activity gradually declined ($p < 0.05$). PGC-1 can regulate mitochondrial metabolism and adaptation through transcriptional regulation, and its decreased expression is a key event in myocardial cell and liver cell necrosis. According to RT-qPCR and Western blotting results, the mRNA and protein levels of PGC-1 in liver cells and myocardial cells in model group were down-regulated compared with those in NC group, while they gradually rose with the increase in the concentration of Daochi Chengqi decoction ($p < 0.05$) as shown in fig. 6.

The results of RT-qPCR and Western blotting showed that the mRNA and protein expressions of TLR4, NF- κ B and p53 in myocardial and liver cells were significantly higher in model group than those in NC group ($p < 0.01$), and they gradually declined with the increase in the concentration of Daochi Chengqi decoction ($p < 0.05$) (fig. 7), consistent with the results of cell experiments.

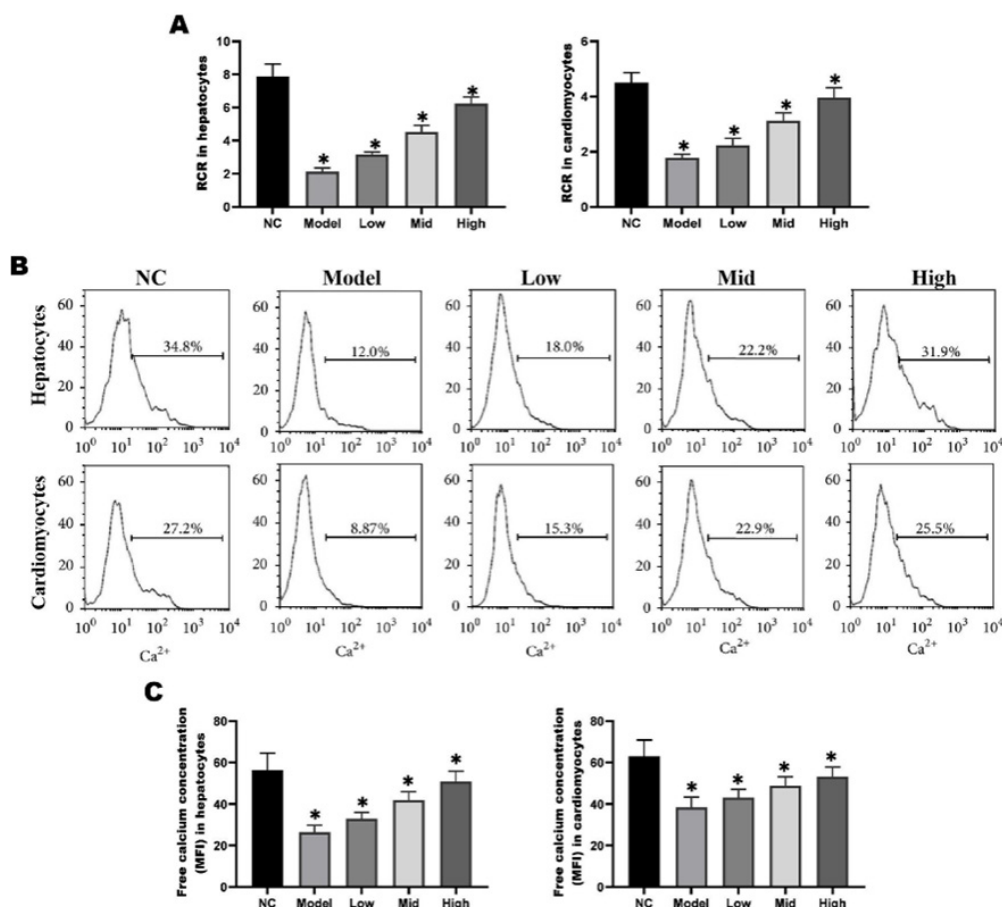


Fig. 4: Daochi Chengqi decoction reversed the decrease of mitochondrial RCR and Ca^{2+} concentration induced by high temperature

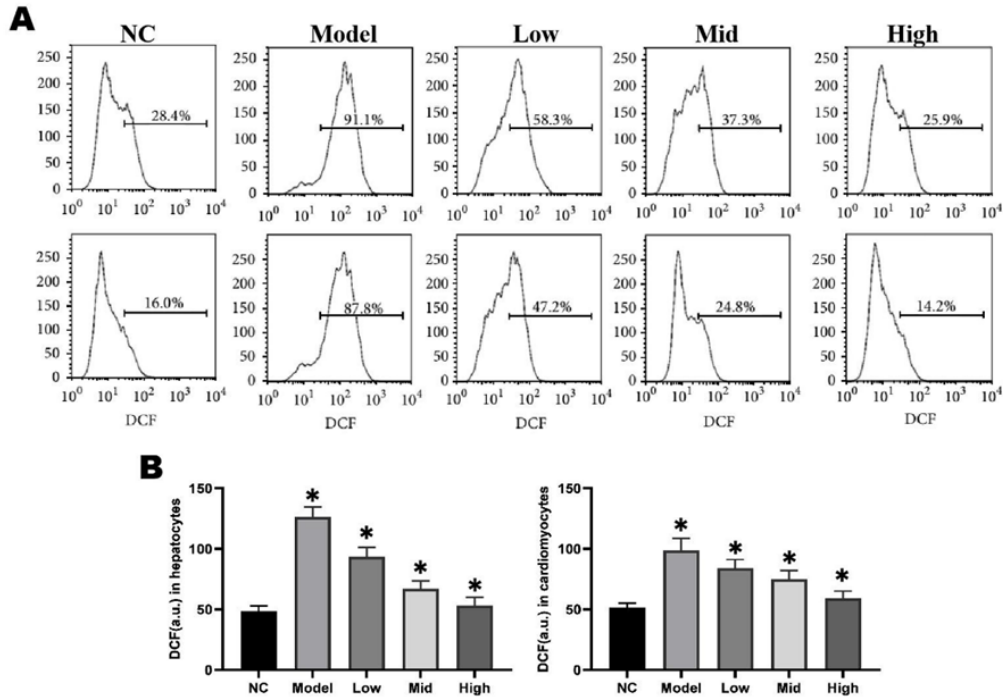


Fig. 5: Daochi Chengqi decoction reversed the increase of mitochondrial ROS level induced by high temperature
 Note: *p<0.05

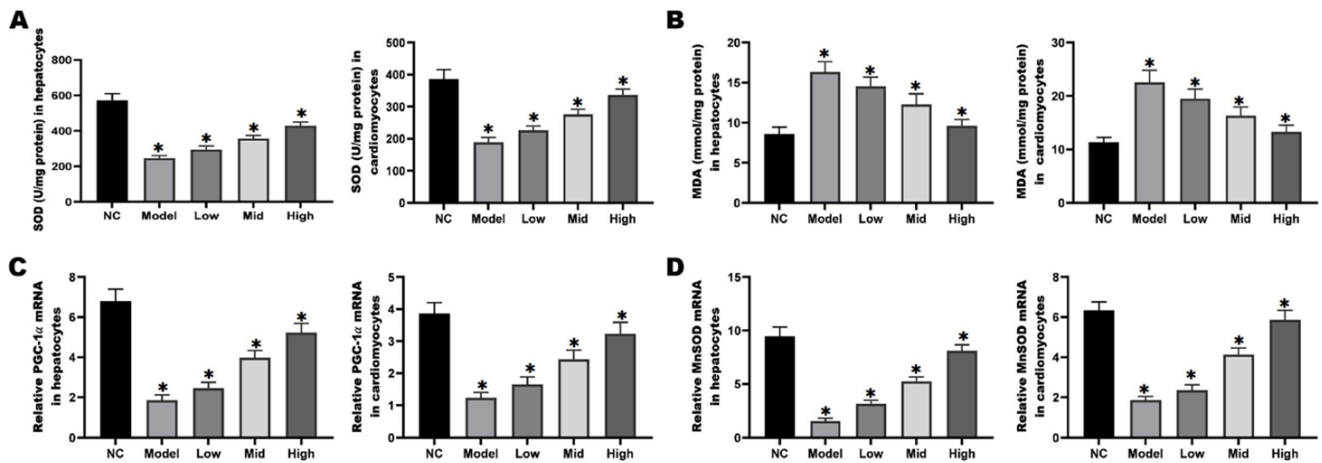


Fig. 6: Effects of Daochi Chengqi decoction on oxidative stress-related factors
 Note: *p<0.05

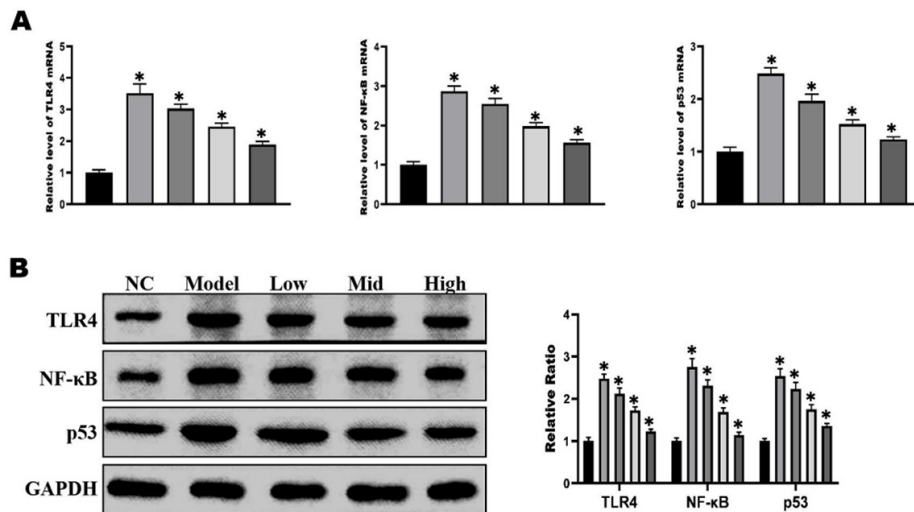


Fig. 7: Inhibitory effect of Daochi Chengqi decoction on TLR4/NF- κ B signaling pathway
 Note: *p<0.05

Summer-heat syndrome is often accompanied by systemic inflammatory responses, which play a key role in myocardial tissue injury. Previous studies have shown that inhibiting inflammatory responses is an important treatment means for myocardial injury caused by summer-heat syndrome^[8]. Skok *et al.*^[9] found that melatonin could protect male rats from heat-induced myocardial injury by relieving oxidative stress and inflammatory response. At present, a large number of studies on the protective effect against myocardial injury induced by summer-heat syndrome are still confined to down-regulation of inflammatory response or oxidative stress, but some experiments have shown^[10,11] that anti-inflammatory therapy alone cannot effectively reverse myocardial injury induced by summer-heat syndrome, suggesting that there may be other injury mechanisms in the process of organ injury induced by summer-heat syndrome. Moreover, according to clinical data^[12], the prognosis of patients who only undergo anti-inflammatory treatment is poor, suggesting that summer-heat syndrome may cause delayed damage to myocardial cells. TLR4 is an important target for the treatment of cardiovascular related diseases, but there are few reports about the mechanism of TLR4 in myocardial injury induced by summer-heat syndrome. In this study, it was found that the expression level of TLR4 in rat myocardial and liver cells was significantly increased after 2 h of culture under high temperature of 43°. Furthermore, the expressions of TLR4/NF-κB pathway-related genes and inflammatory factors TNF-α, IL-6 and IL-1β were also significantly increased. TLR4 is a pattern-recognition receptor that can regulate multiple cell death modes in myocardial tissues, including inflammation, apoptosis, autophagy and ferroptosis^[13]. The TLR4/NF-κB signaling pathway is an important inflammatory signaling pathway, which is involved in the pathophysiological processes of cardiovascular diseases such as cardiac ischemia, ventricular remodeling, fibrosis and heart failure^[14]. It has been reported^[15] that in elderly patients with chronic heart failure plus pulmonary infection, the TLR4/NF-κB signaling pathway in peripheral blood is significantly activated, and the expression levels of inflammatory factors such as IL-4, IL-6 and TNF-α are significantly increased. Blocking the TLR4/NF-κB signaling pathway may help to relieve post-coronary microembolization myocardial injury and improve cardiac function. These results suggest that inhibiting the TLR4/NF-

κB signaling pathway can ameliorate mitochondrial damage caused by high temperature in myocardial cells, thus protecting cell function. In this study, it was found that the mRNA and protein levels of TLR4, NF-κB and p53 in *in vitro* cell models and rat myocardial and liver cells declined gradually with the increase in the concentration of Daochi Chengqi decoction, indicating that the TLR4/NF-κB signaling pathway may be an important target of Daochi Chengqi decoction in the treatment of summer-heat syndrome.

MMP refers to the difference in charge between the inside and outside of the mitochondrial membrane. Under normal circumstances, the inner side of mitochondrial membrane has negative charges, while the outer side has positive charges, forming a voltage difference between the inside and outside of the membrane, which can drive the energy conversion inside mitochondria and maintain normal cellular metabolism^[16]. MMP will be altered in the case of cell stress or injury. If the MMP is too low, mitochondrial dysfunction will be caused, and many harmful chemicals will be released, inducing cell death. In this study, the mean MMP in myocardial and liver cells in model group declined significantly compared with that in NC group, while it rose gradually with the increase in the concentration of Daochi Chengqi decoction. SOD is an antioxidant enzyme that can convert superoxide radicals into oxygen and hydro peroxide, thereby reducing oxidative injury^[17]. MDA is one of the products of oxidative injury, which may affect mitochondrial function by oxidizing lipids and proteins. It has been found that the decrease in SOD activity in muscle mitochondria of aged rats is significantly correlated with the decline in mitochondrial function^[18]. At the same time, the polymorphism of SOD gene may be related to human mitochondrial dysfunction. Besides, MDA can negatively affect mitochondrial function, and it can damage mitochondrial membrane structure and function by oxidizing mitochondrial lipids and may also destroy the function of mitochondrial enzymes by oxidizing mitochondrial proteins. In this study, the results of ELISA revealed that compared with NC group, model group had significantly decreased SOD activity in mitochondria and significantly increased MDA activity. With the increase in the concentration of Daochi Chengqi decoction, the SOD activity in mitochondria of myocardial and

liver cells gradually rose, and the MDA activity gradually declined. It can be inferred that Daochi Chengqi decoction can protect the mitochondrial function of myocardial and liver cells by inhibiting the production of oxidative stress-related factors.

PGC-1 is a transcriptional coactivator able to regulate mitochondrial metabolism and adaptation through transcription, which has important effects on mitochondrial biosynthesis, mitochondrial function regulation, MMP maintenance and mitochondrial respiratory chain complex assembly. The decrease in the expression of PGC-1 is a key event of myocardial cell and liver cell necrosis^[19]. In addition, PGC-1 can also control the number and morphology of mitochondria by regulating mitochondrial dynamic processes, enhance mitochondrial fusion and fission, and maintain mitochondrial integrity and homeostasis^[20]. In this study, according to RT-qPCR and Western blotting results, the mRNA and protein levels of PGC-1 in liver cells and myocardial cells in model group were down-regulated compared with those in NC group, while they gradually rose with the increase in the concentration of Daochi Chengqi decoction. These findings suggest that Daochi Chengqi decoction can increase mitochondrial DNA replication and transcription by increasing the PGC-1 expression, thereby enhancing mitochondrial biosynthesis.

In conclusion, Daochi Chengqi decoction can reduce mitochondrial oxidative damage through inhibiting the activity of the TLR4/NF- κ B signaling pathway, thereby reversing the acute phase progression of summer-heat syndrome of epidemic febrile disease in rats.

Funding:

The work was supported by Startup Found for scientific research, Fujian Medical University (Grant number: 2021QH1041).

Author contributions:

Shenglu Lin and Huiling Yu contributed equally to this work.

Conflict of interests:

The authors declared no conflict of interests.

REFERENCES

1. Kong C, Song W, Fu T. Systemic inflammatory response syndrome is triggered by mitochondrial damage. *Mol Med Rep* 2022;25(4):1-8.

2. Zhu Y, Ma S, Deng HY, Wu Y, Zhang J, Xiang XM, *et al.* The characteristics of organ function damage of hemorrhagic shock in hot environment and the effect of hypothermic fluid resuscitation. *Shock* 2022;57(4):526-35.
3. Li L, Tan H, Zou Z, Gong J, Zhou J, Peng N, *et al.* Preventing necroptosis by scavenging ROS production alleviates heat stress-induced intestinal injury. *Int J Hyperthermia* 2020;37(1):517-30.
4. Kwong S, Meyerson C, Zheng W, Kassardjian A, Stanzione N, Zhang K, *et al.* Acute hepatitis and acute liver failure: Pathologic diagnosis and differential diagnosis. *Semin Diagn Pathol* 2019;36(6):404-14.
5. Wu M, Wang C, Zhong L, Liu Z. Serum myoglobin as predictor of acute kidney injury and 90-day mortality in patients with rhabdomyolysis after exertional heatstroke: An over 10-year intensive care survey. *Int J Hyperthermia* 2022;39(1):446-54.
6. Sun Z, Wang L, Han L, Wang Y, Zhou Y, Li Q, *et al.* Functional calsequestrin-1 is expressed in the heart and its deficiency is causally related to malignant hyperthermia-like arrhythmia. *Circulation* 2021;144(10):788-804.
7. Chen GD, Fan H, Zhu JH. Salidroside pretreatment protects against myocardial injury induced by heat stroke in mice. *J Int Med Res* 2019;47(10):5229-38.
8. Odagiri A, Yamaoka A, Miyata K, Bunya N, Kasai T, Takeyama Y, *et al.* Elderly-onset acute necrotizing encephalopathy mimicking severe heat stroke: A case report and review of the literature. *Acute Med Surg* 2019;6(3):316-20.
9. Skok K, Duh M, Stožer A, Markota A, Gosak M. Thermoregulation: A journey from physiology to computational models and the intensive care unit. *Wiley Interdiscip Rev Syst Biol Med* 2021;13(4):e1513.
10. Huang W, Xie W, Gong J, Wang W, Cai S, Huang Q, *et al.* Heat stress induces RIP1/RIP3-dependent necroptosis through the MAPK, NF- κ B, and c-Jun signaling pathways in pulmonary vascular endothelial cells. *Biochem Biophys Res Commun* 2020;528(1):206-12.
11. Kruijt N, den Bersselaar LV, Snoeck M, Kramers K, Riazi S, Bongers C, *et al.* RYR1-related rhabdomyolysis: A spectrum of hypermetabolic states due to ryanodine receptor dysfunction. *Curr Pharm Design* 2022;28(1):2-14.
12. Wang L, Deng Z, Yuan R, Zhao Y, Yang M, Hu J, *et al.* Protective effect and mechanism of mesenchymal stem cells on heat stroke induced intestinal injury. *Exp Ther Med* 2020;20(4):3041-50.
13. Chen H, Lin X, Yi X, Liu X, Yu R, Fan W, *et al.* SIRT1-mediated p53 deacetylation inhibits ferroptosis and alleviates heat stress-induced lung epithelial cells injury. *Int J Hyperthermia* 2022;39(1):977-86.
14. Liu Z, Zhao J, Sun R, Wang M, Wang K, Li Y, *et al.* *Lactobacillus plantarum* 23-1 improves intestinal inflammation and barrier function through the TLR4/NF- κ B signaling pathway in obese mice. *Food Function* 2022;13(11):5971-86.
15. Xu X, Piao HN, Aosai F, Zeng XY, Cheng JH, Cui YX, *et al.* Arctigenin protects against depression by inhibiting microglial activation and neuroinflammation via HMGB1/TLR4/NF- κ B and TNF- α /TNFR1/NF- κ B pathways. *Br J Pharmacol* 2020;177(22):5224-45.
16. Ding Y, Wang L, Zhao Q, Wu Z, Kong L. microRNA-93 inhibits chondrocyte apoptosis and inflammation in osteoarthritis by targeting the TLR4/NF- κ B signaling pathway. *Int J Mol Med* 2019;43(2):779-90.

17. Filipe A, Chernorudskiy A, Arbogast S, Varone E, Villar-Quiles RN, Pozzer D, *et al.* Defective endoplasmic reticulum-mitochondria contacts and bioenergetics in SEP1-related myopathy. *Cell Death Differ* 2021;28(1):123-38.
 18. Goto H, Shoda S, Nakashima H, Noguchi M, Imakiire T, Ohshima N, *et al.* Early biomarkers for kidney injury in heat-related illness patients: A prospective observational study at Japanese Self-Defense Force Fuji Hospital. *Nephrol Dial Transplant* 2023;38(3):644-54.
 19. Xie W, Huang W, Cai S, Chen H, Fu W, Chen Z, *et al.* NF- κ B/I κ B α signaling pathways are essential for resistance to heat stress-induced ROS production in pulmonary microvascular endothelial cells. *Mol Med Rep* 2021;24(5):1-8.
 20. Lakmali JP, Thirumavalavan K, Dissanayake D. A rare case of posterior reversible encephalopathy syndrome in a patient with severe leptospirosis complicated with rhabdomyolysis and acute kidney injury; a case report. *BMC Infect Dis* 2021;21(1):522.
-